



ELSEVIER

Journal of Crystal Growth 175/176 (1997) 741–746

---

---

JOURNAL OF **CRYSTAL  
GROWTH**

---

---

# Growth controlled fabrication and cathodoluminescence study of 3D confined GaAs volumes on non-planar patterned GaAs(0 0 1) substrates

A. Konkar\*, H.T. Lin, D.H. Rich, P. Chen, A. Madhukar

*Photonic Materials and Devices Laboratory, Department of Materials Science and Engineering, University of Southern California, Los Angeles, California 90089-0241, USA*

---

## Abstract

We report on (a) the effect of growth interruption on the growth profile evolution in growth on non-planar patterned mesa tops via substrate-encoded size-reducing epitaxy (SESRE) and (b) the optical behavior of isolated 3D-confined GaAs volumes as well as 3D-confined GaAs volumes coupled with 1D-confined quantum wells (QWs) fabricated by SESRE. Steady-state excitation and time-resolved cathodoluminescence (CL) are used for these optical studies.

*Keywords:* Patterned substrate; Growth interruption; Quantum boxes; Time-resolved cathodoluminescence

---

## 1. Introduction

The fabrication of semiconductor structures with electronic states confined in more than one dimension is a subject of much activity in recent years. Of the various approaches to the fabrication of such structures, in situ, one-step growth approaches are promising since the structures thus fabricated are expected to be devoid of the problems of damage and contamination. Substrate-encoded size-reducing epitaxy [1] is one such in situ approach in which the differential growth rates on various facets

and inter-facet adatom migration are exploited to reduce the mesa top size from as-patterned length scales (typically 1  $\mu\text{m}$ ) down to the nanoscale ( $< 100 \text{ nm}$ ) regime. One of the critical issues in this approach is the growth condition dependence of the growth profile evolution. Previous studies [1–3] of the growth condition dependence of the growth profile evolution have been limited to the case of continuous growth. In this paper we report on some findings on the effect of growth interruption on the growth on stripe mesas on GaAs(0 0 1). Additionally, 3D confined GaAs volumes synthesized on  $< 1 0 0 >$  oriented square mesas [3] via SESRE are examined via steady state as well as time-resolved CL studies to shed light on carrier dynamics of significance to carrier collection

---

\* Corresponding author.

efficiency in isolated or communicating 3D-confined volumes.

## 2. Experimental procedure

GaAs  $(001) \pm 0.1^\circ$  substrates were patterned via conventional photolithography followed by wet chemical etching. The effect of growth interruption was studied for growth on stripe mesas oriented along the  $\langle 100 \rangle$  and  $[1\bar{1}0]$  directions, with mesa width of  $\sim 1 \mu\text{m}$  and depth of  $\sim 0.5 \mu\text{m}$ . The growth interruption used in these experiments has a duration of  $\sim 120$  s. GaAs layers of 45 ML thickness followed by 5 ML AlGaAs marker layers were grown to reveal the growth profile evolution. Square mesas for the fabrication of 3D-confined GaAs volumes were patterned along  $\langle 100 \rangle$  directions. The details of the substrate preparation, MBE growth procedures and the growth profile evolution for 3D-confined GaAs volumes have been given in an earlier paper [3]. For the samples with interacting 3D-confined GaAs volumes and 2D-confined GaAs QWs, the MBE growth consisted of a size-reducing buffer of four periods of  $[175 \text{ ML Al}_{0.25}\text{Ga}_{0.75}\text{As}/525 \text{ ML GaAs}]$  followed by a 40 period multiple quantum well (MQW) composed of  $[40 \text{ ML Al}_{0.25}\text{Ga}_{0.75}\text{As}/20 \text{ ML GaAs}]$ . For the sample containing isolated

3D-confined GaAs volumes, the growth consisted a size-reducing buffer composed of 16 period of  $[5 \text{ ML Al}_{0.25}\text{Ga}_{0.75}\text{As}/195 \text{ ML GaAs}]$  followed by  $100 \text{ ML Al}_{0.25}\text{Ga}_{0.75}\text{As}/20 \text{ ML GaAs}/200 \text{ ML Al}_{0.25}\text{Ga}_{0.75}\text{As}$  and capped by 50 ML GaAs.

The CL studies were performed with a modified JEOL-840A scanning electron microscope (SEM) with a 0.25 m monochromator. Time-resolved CL experiments were performed with the method of delayed coincidence in an inverted single photon counting mode with a time resolution of  $\sim 100$  ps [4]. Electron beam pulses of 50 ns width and a frequency 1 MHz were used for excitation for the time-resolved studies.

## 3. Results and discussion

### 3.1. Effect of growth interruption on the growth profile evolution

In Fig. 1 are presented the transmission electron microscope (TEM) images showing the growth profile evolution on stripe mesas along the  $[1\bar{1}0]$  (parallel to the As dimer direction; panels (a) and (b)) and the  $[010]$  (at  $45^\circ$  to the As dimer direction; panels (d) and (e)) directions for different temperatures. The  $\text{As}_4$  pressure is kept constant at  $4.8 \times 10^{-6}$  Torr and the GaAs growth rate at

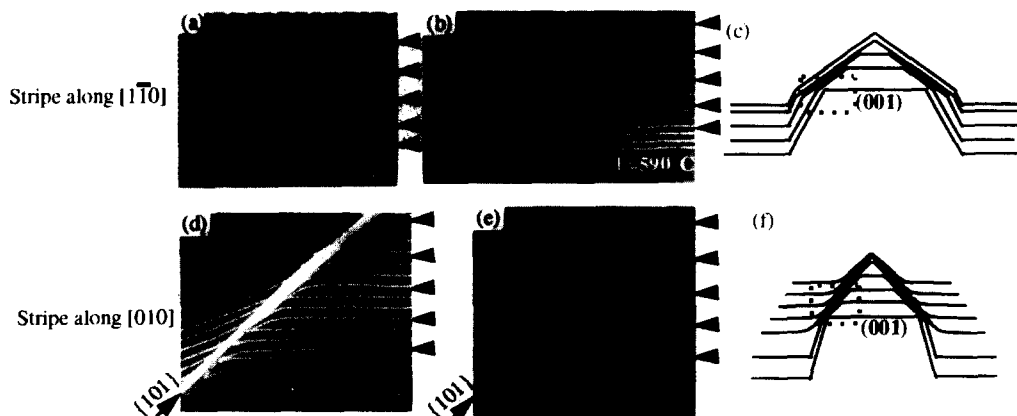


Fig. 1. TEM images of growth on stripe mesas: (a) and (b) along  $[1\bar{1}0]$  direction, (d) and (e) along  $[010]$  direction. Schematic drawings of the growth profile evolution are shown in panels (c) and (f) for the stripe mesas along  $[1\bar{1}0]$  and  $[010]$  directions, respectively.

0.5 ML/s. Only a portion of the mesa top and sidewalls is shown in these images corresponding to the area marked by the dotted rectangle in the schematic drawings in panels (c) and (f). The thin white lines are the AlGaAs markers which delineate the growth profile. The arrows indicate the GaAs layers in which growth was interrupted.

In the case of the growth on stripe mesas along the  $[1\bar{1}0]$  direction, layer thickness on the mesa top (sidewall) for the GaAs layers in which the growth was interrupted is found to be higher (lower) than the preceding and following layers. This implies that migration of Ga atoms from the sidewalls to the mesa top continues in the absence of Ga delivery. Careful measurements of these layer thicknesses for the growth at  $610^\circ\text{C}$  indicate that more than 1 ML worth of material migrated from the sidewalls. This indicates that during growth interruption it is not only the initial adatoms on the sidewalls but the atoms that were incorporated into the sidewalls during the growth also migrate to the mesa top. The effect of interruption on the growth profile evolution becomes less significant when the substrate temperature is lowered to  $590^\circ\text{C}$ . The flat morphology on the mesa top as evidenced by the AlGaAs markers implies that the migration length of the adatoms on the mesa top, perpendicular to the stripe direction, is larger than half the mesa width (i.e. the migration length is at least  $\sim 0.5\ \mu\text{m}$  for the growth condition used).

Unlike the above case, in the case for the growth on stripe mesas along  $[010]$  direction at  $610^\circ\text{C}$  the thickness on the mesa top of the GaAs layers for which the growth was interrupted is found to be lower than the preceding and following layers (which is evident for the first two interruptions in panel (d)). This implies that in this case Ga atoms migrate in the opposite direction, i.e. from the mesa top to the sidewalls in the absence of Ga delivery. Moreover, a curved morphology is present at the intersection of the mesa top and sidewalls for the GaAs layers with growth interruption. Again, the effect of interruption on the growth profile evolution becomes less significant when the substrate temperature is lowered to  $590^\circ\text{C}$ .

### 3.2. CL studies of 3D-confined GaAs volumes

#### 3.2.1. Interacting 3D-confined GaAs volumes and 1D-confined quantum wells (QWs)

Fig. 2 shows a TEM image of a typical square mesa containing interacting 3D-confined GaAs volumes (dark regions) on the mesa top below pinch-off and 1D-confined GaAs QWs on the  $\{101\}$  sidewalls. The area-averaged CL spectra, taken from a region  $\sim 1\ \mu\text{m} \times 1\ \mu\text{m}$  centered on the mesa top [5], at various sample temperatures are shown in Fig. 3. The spatial region responsible for the identifiable peaks in Fig. 3 can be inferred from the spatially resolved monochromatic CL images and the SEM image shown in Fig. 4. The luminescence from p1 and p2 is primarily from QWs grown on sidewalls away from mesa top while p3 is localized about the mesa top and hence is from thick 3D-confined GaAs volumes just below the pinch-off region. Peak p4 is similarly identified to be from the underlying bulk-like GaAs in the size-reducing buffer.

The peak intensity decrease of p1 relative to p2 and p3 with increasing temperature seen in Fig. 3 indicates thermal re-emission of carriers from thinner QWs (p1) and their subsequent transport and recombination in the thicker QW (p2) and the 3D-confined volumes (p3). Further insight into these thermalization effects is gained from the time-delayed CL measurements. The intensity of peaks p1–p4 ( $I_{pi}$ ) as a function of time ( $t$ ) for both decay and onset stages is shown in Fig. 5a and b, respectively. The onset rate  $r$ , defined as  $\Delta \ln(I_{pi})/\Delta t$ ,



Fig. 2. TEM image of a 20 ML GaAs/40 ML AlGaAs multiple QW growth on the mesa top.

is the slowest for p4 (see Fig. 5b) reflecting the large distances ( $\sim 0.5 \mu\text{m}$ ) that the hot carrier must traverse before recombining in the thick bulk-like GaAs layers in the size-reducing buffer. These

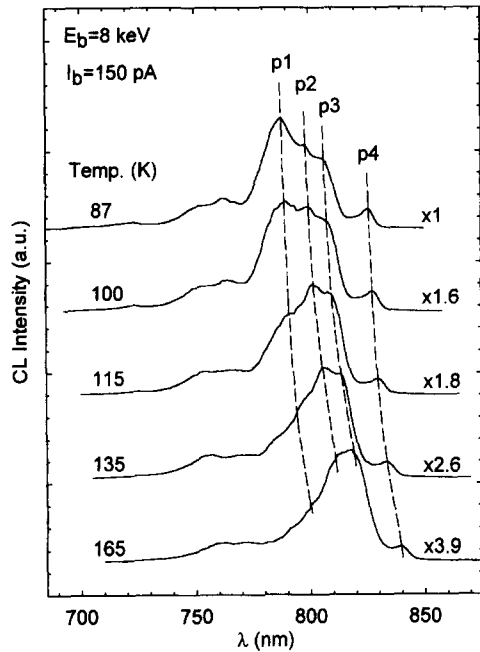


Fig. 3. Constant excitation CL spectra taken at various temperatures. The peak shifts for p1 to p4 with temperature are shown by dashed lines.

relative rates are also observed in Fig. 5c from the peak intensity ratios. The initial decay time  $\tau_1$  measured from the slopes in the  $\ln(I_{pi})$  versus time transients shown in Fig. 5a increases in the order p1, p2 and p3 implying the enhanced thermal re-emission of carriers in the QWs (p1 and p2) to feed continuously the larger 3D-confined GaAs volumes represented by p3, as the system proceeds towards equilibrium.

### 3.2.2. Isolated 3D-confined GaAs volumes

Fig. 6a shows a TEM image of growth of the SQW on the square mesa top. As seen in the figure, the mesa top size at the start of the GaAs well deposition is  $\sim 120 \text{ nm}$ . The thickness of the GaAs layer on the mesa top ( $\sim 11 \text{ nm}$ ) is higher compared to the deposition thickness ( $\sim 5.7 \text{ nm}$ ) due to adatom migration from the  $\{101\}$  sidewalls to the  $(001)$  mesa top. Negligible GaAs growth on the  $\{101\}$  sidewalls in the vicinity of the 3D-confined volume is observed indicating good lateral confinement.

Results from CL imaging and spectroscopy are shown in Fig. 6 (panels (c) and (d)) and Fig. 7, respectively. The monochromatic CL images (Fig. 6) show that the high energy peak seen in the spectra shown in Fig. 7 is associated with 3D-confined GaAs volume and the low energy peak has its origin in the bulk-like GaAs in the size-reducing buffer layer. The CL spectra from the

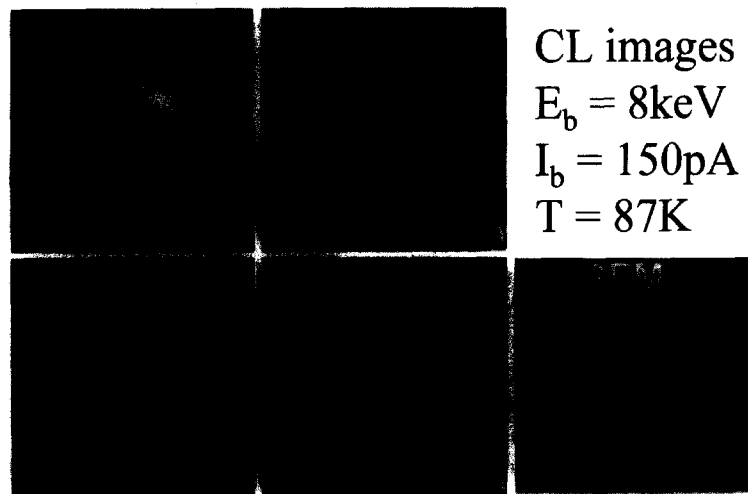


Fig. 4. Monochromatic CL images at various wavelengths (a)–(d), and (e) SEM image. The arrow tips point to the mesa apex position. CL imaging conditions are indicated in the upper right corner.

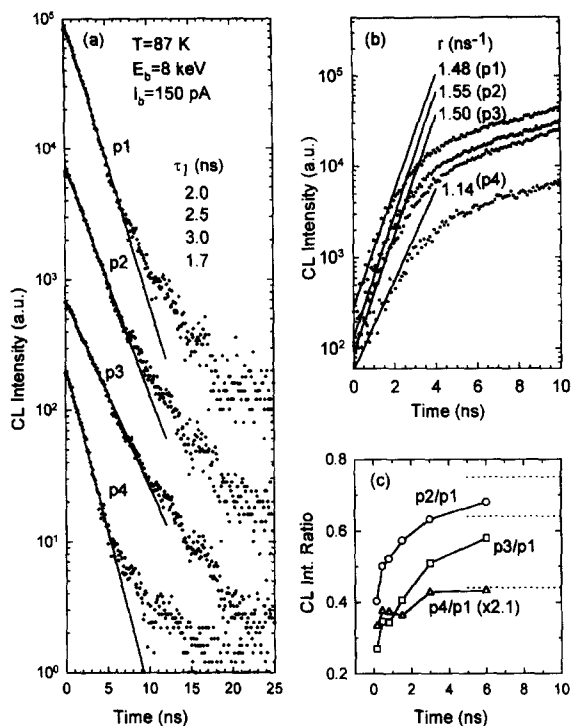


Fig. 5. CL transients for peaks p1–p4: (a) the decay curves with linear fits for the initial  $\sim 6$  ns of decay; (b) the onset curves with linear fits for the first  $\sim 2$  ns; (c) CL peak intensity ratios p2/p1, p3/p1, and p4/p1.

non-patterned planar region (not shown) shows a peak at  $\lambda = 778$  nm at 87 K which is associated with the SQW deposition. The red shift of the CL peak from well deposition on the mesa top with respect to that from the planar region is attributed to interfacet adatom migration induced GaAs thickness enhancement on the mesa top. The temperature dependence of the CL spectra (see Fig. 7) shows that the ratio of the peak intensity of the 3D-confined to bulk-like GaAs decreases with increasing temperature ( $T < 90$  K) indicating good carrier confinement in these 3D-confined volumes. The reversal of this trend for temperatures beyond 90 K is under investigation.

Strong evidence for 3D confinement of the high energy peak in the CL spectra comes from the results of excitation current dependence. Fig. 8 shows a plot of the full width at half maximum

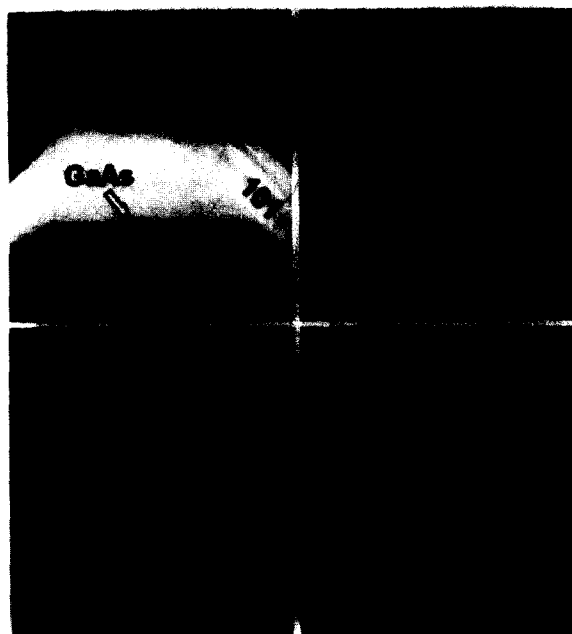


Fig. 6. (a) TEM, (b) SEM, and monochromatic CL images at (c)  $\lambda = 810$  nm and (d)  $\lambda = 822$  nm taken with an electron beam of  $E_b = 8$  keV and  $I_b = 150$  pA at  $T = 87$  K. The length scale for the CL images (c) and (d) is indicated in the SEM image. The arrow tips in (b)–(d) point to the mesa apex position.

(FWHM) versus the excitation current for the peaks from the mesa top 3D confined GaAs volume (labeled mesa) and the corresponding GaAs/AlGaAs single QW (SQW) in the planar region (labeled planar) of the same sample. The FWHM of the SQW on the planar region increases from  $\sim 6.7$  to  $\sim 9.6$  meV as  $I_b$  increases from 10 pA to 5 nA, whereas the FWHM of the 3D-confined region increases by a factor of almost 3 for the same increase of  $I_b$ . This enhanced peak width broadening reflects rapid phase-space-filling in the 3D-confined GaAs volume.

#### 4. Conclusion

The role of growth interruption during SESRE on patterned stripe mesas is examined for the first time and found to reveal remarkable continued interfacet migration during growth interruption.

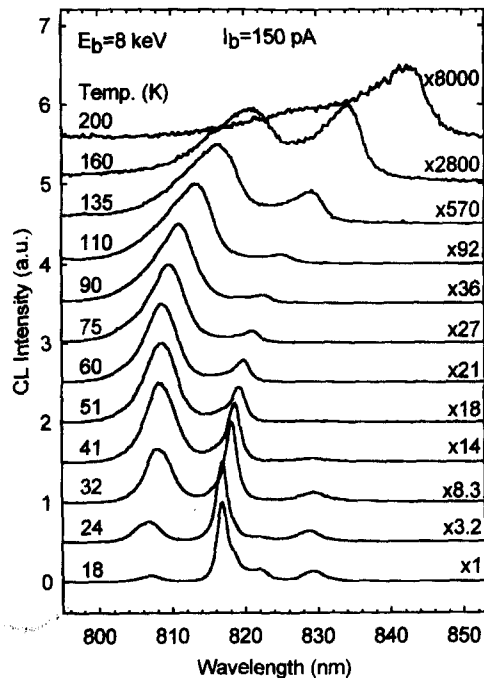


Fig. 7. Constant excitation CL spectra taken at various temperatures in  $18 \text{ K} \leq T \leq 200 \text{ K}$  range.

Temperature-dependent and time-resolved CL experiments on coupled 3D-confined volumes grown by SESRE reveal carrier feeding from sidewall quantum wells to the 3D-confined volumes. Isolated confined 3D volumes show the expected phase-space-filling behavior.

#### Acknowledgements

This work was supported by AFOSR, ONR, and NSF (RIA-ECS).

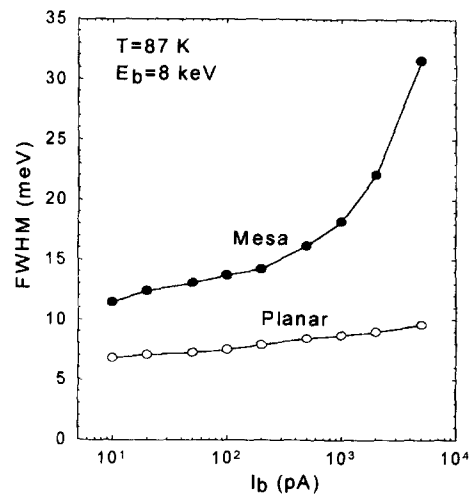


Fig. 8. Full width at half maximum (FWHM) of CL peaks originating from the 3D-confined GaAs volume and the GaAs/AlGaAs single QW (denoted as mesa and planar, respectively) as a function of excitation current.

#### References

- [1] A. Madhukar, K.C. Rajkumar and P. Chen, Appl. Phys. Lett. 62 (1993) 1547; A. Madhukar, Thin Solid Films 231 (1993) 8.
- [2] See, for example: M. Lopez and Y. Nomura, J. Crystal Growth 150 (1995) 68, and references therein.
- [3] A. Konkar, K.C. Rajkumar, Q. Xie, P. Chen, A. Madhukar, H.T. Lin and D.H. Rich, J. Crystal Growth 150 (1995) 311.
- [4] D. Bimberg, H. Munzel, A. Steckenborn and J. Christen, Phys. Rev. B 31 (1985) 7788.
- [5] D.H. Rich, H.T. Lin, A. Konkar, P. Chen and A. Madhukar, Appl. Phys. Lett. 69 (1996) 665.